TRANSACTIONS ON ELECTRICAL AND ELECTRONIC MATERIALS
Vol. 16, No. 6, pp. 342-345, December 25, 2015

Regular Paper

pISSN: 1229-7607 eISSN: 2092-7592
DOI: http://dx.doi.org/10.4313/TEEM.2015.16.6.342
OAK Central: http://central.oak.go.kr

Thermoelectric Properties of n-Type Half-Heusler Compounds Synthesized by the Induction Melting Method

Nguyen Van Du
Energy & Environmental Materials Division, Korea Institute of Ceramic Engineering & Technology, Jinju 52861, and School of Advanced Material Engineering, Changwon National University, Changwon 51140, Korea

Soonil Lee†, Won-Seon Seo, Nguyen Minh Dat, Eun-Ji Meang, and Chang-Hyun Lim
Energy & Environmental Materials Division, Korea Institute of Ceramic Engineering & Technology, Jinju 52861, Korea

Jamil Ur Rahman
Energy & Environmental Materials Division, Korea Institute of Ceramic Engineering & Technology, Jinju 52861, and School of Advanced Material Engineering, Changwon National University, Changwon 51140, Korea

Myong Ho Kim
School of Advanced Material Engineering, Changwon National University, Changwon 51140, Korea

Received November 20, 2015; Accepted November 23, 2015

The *n*-type $Hf_{0.25}Zr_{0.25}Ti_{0.5}NiSn_{0.998}Sb_{0.002}$ Half-Heusler (HH) alloy composition was prepared by using the induction melting method in addition to the mechanical grinding, annealing, and spark plasma sintering processes. Analysis of X-ray diffraction (XRD) results indicated the formation of a pure phase HH structured compound. The electrical and thermal properties at temperatures ranging from room temperature to 718 K were investigated. The electrical conductivity increased with increasing temperatures and demonstrated nondegenerate semiconducting behavior, and a large reduction in the thermal conductivity to the value of 2.5 W/mK at room temperature was observed. With the power factor and thermal conductivity, the dimensionless figure of merit was increased with temperature and measured at 0.94 at 718 K for the compound synthesized by the induction melting process.

Keywords: Thermoelectric, Half-Heusler, Induction melting, Thermal property, Charge transport

1. INTRODUCTION

With their improved figure of merit and the recent developments in nanotechnology, thermoelectric materials have attracted more attention given their potential applications in electronic cooling, special power generation, waste heat recovery, etc. [1-3]. The conversion efficiency of a thermoelectric material is related to the dimensionless figure of merit, $ZT= \alpha^2\sigma T/\kappa$, where α, σ, κ, and T are the Seebeck coefficient, electrical conductivity, total thermal conductivity and absolute temperature, respectively. Prior studies on thermoelectric materials have been published with ZT diversity values varying based on different operating temperatures, such as Bi_2Te_3 for low temperature [4-6], PbTe

† Author to whom all correspondence should be addressed:
E-mail: leesoonil@gmail.com

for mid-temperature [7-9], Skutterudites and HHs for mid-high temperature [10,11]. HH compounds are known to be relatively stable at high temperature despite their complex compositions. Based on the figure of merit for MNiSn (M = Hf, Zr, Ti) materials, Sakurada *et al.* reported the highest ZT value of 1.5 at 673 K for a $Hf_{0.25}Zr_{0.25}Ti_{0.5}NiSn_{0.998}Sb_{0.002}$ composition in 2005 [11,12], but the ZT value has not been reproducible to date. Recently, Schwall *et al.* (2013) reported ZT=1.2 at 830 K with a similar composition and synthetic method by using the arc melting process. The arc melting process has been generally used for the HH compounds due to the high melting temperature. In the present study, we investigated the thermoelectric properties with a novel synthetic approach using the induction melting method to prepare the $Hf_{0.25}Zr_{0.25}Ti_{0.5}NiSn_{0.998}Sb_{0.002}$ composition with the goal of maximizing the ZT value of this system.

2. EXPERIMENTS

A Half-Heusler composition of $Hf_{0.25}Zr_{0.25}Ti_{0.5}NiSn_{0.998}Sb_{0.002}$ was chosen for investigation. The raw materials used in this work include Hf powder (99.6%, Alfa Aesar), Zr foil (99.5%, Alfa Aesar), Ti powder (99.9%, Alfa Aesar), Ni powder (99.8%, Alfa Aesar) and Sn ingot (2mm dia. x 5mm long, 99.99%, RNP Korea), Sb (99.999%, High Purity Chemical) with shape of grains ca. 2 mm. All the elements were weighed in the correct proportion to synthesize a compound composed of $Hf_{0.25}Zr_{0.25}Ti_{0.5}NiSn_{0.998}Sb_{0.002}$. The raw materials were placed in a quartz tube, which was coated with a thin carbon layer to prevent reaction with the inner wall of the quartz tube at high temperatures and sealed under 2×10^{-2} Torr. The mixture was melted using an RF induction furnace for 30 minutes to form the ingot. The ingots were then ground into powder by using a motorized mortar and pestle to ensure homogeneity before encapsulating the contents into a quartz tube once again with the vacuum inside. The encapsulated sample was annealed at 1173 K for 5 days to transform the materials into a pure phase. After annealing, the sample was ground again and sieved with a 35 μm-mesh sieve. The powder was then sintered by Spark Plasma Sintering (SPS) at 1,273 K for 1 hour under a pressure of 60 MPa using a graphite mold to form the cylinder shape ((*Φ*) 12.5 mm × (H) 7 mm). Samples with the dimensions of 3×3×10 mm3 (sample A), (H) 1.5 mm × (*Φ*) 12.5 mm (sample B), (H) 1.0 mm × (*Φ*) 12.5 mm (sample C) were cut from a cylinder to carry out the structural, electrical, and thermal property measurements. The phase composition was analyzed by x-ray diffraction (XRD) using the Rigaku D/MAX-2500/PC with Cu Kα radiation on three samples: the powder sample after melting; after annealing at 1,173 K in 5 days; and sample C. The specific heat was measured with a differential scanning calorimeter and the density was determined using the Archimedes' method. The thermal diffusivity of sample B was measured by a laser flash method (DLF-1300, TA instrument). The electrical conductivity and Seebeck coefficient of sample A were measured by a thermoelectric property measurement system (RZ2001i, Ozawa Science, Japan).

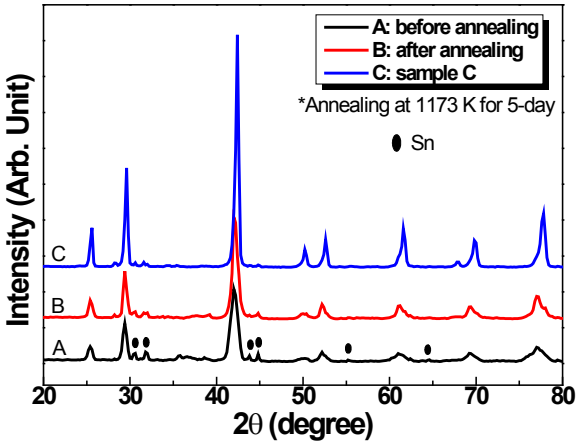

Fig. 1. XRD patterns of $Hf_{0.25}Zr_{0.25}Ti_{0.5}NiSn_{0.998}Sb_{0.002}$ sample before and after annealing, and after SPS (sample C) process.

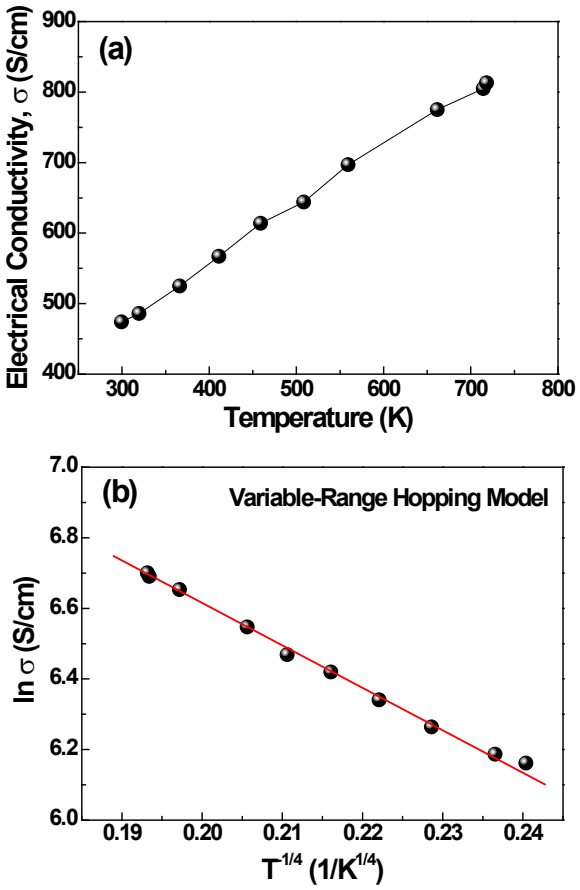

Fig. 2. (a) Temperature dependence of the electrical conductivity and (b) plot of ln σ vs. $T^{1/4}$ of $Hf_{0.25}Zr_{0.25}Ti_{0.5}NiSn_{0.998}Sb_{0.002}$ sample.

3. RESULTS AND DISCUSSION

The x-ray diffraction patterns for the $Hf_{0.25}Zr_{0.25}Ti_{0.5}NiSn_{0.998}Sb_{0.002}$ powders before annealing, after annealing, and after SPS (sample C) are shown in Fig. 1. With powder sample before annealing formed the major phase with a Half-Heusler type structure, but a small amount of Sn was observed and disappeared after the annealing process, as shown in Fig. 1B. The HH single phase was observed more clearly with the sample following SPS, as shown in Fig. 1C. This validates the strong influence of annealing and the SPS processes on the forming of the single-phase structure of the $Hf_{0.25}Zr_{0.25}Ti_{0.5}NiSn_{0.998}Sb_{0.002}$ compound.

Figure 2 shows the variations in electrical conductivity as a function of temperature. As shown in Fig. 2(a), the electrical conductivity increases linearly when the temperature increases from room temperature (RT) to 718 K, indicating a nondegenerate semiconductor-like behavior with increase

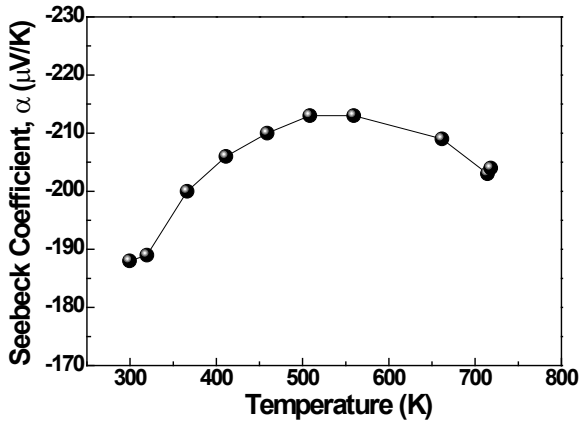

Fig. 3. Temperature dependence of the Seebeck coefficient of $Hf_{0.25}Zr_{0.25}Ti_{0.5}NiSn_{0.998}Sb_{0.002}$ sample from RT to 718 K.

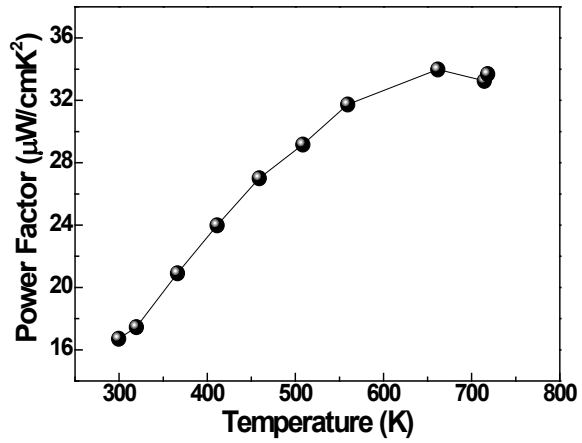

Fig. 4. Temperature dependence of the power factor of $Hf_{0.25}Zr_{0.25}Ti_{0.5}NiSn_{0.998}Sb_{0.002}$ sample from RT to 718 K.

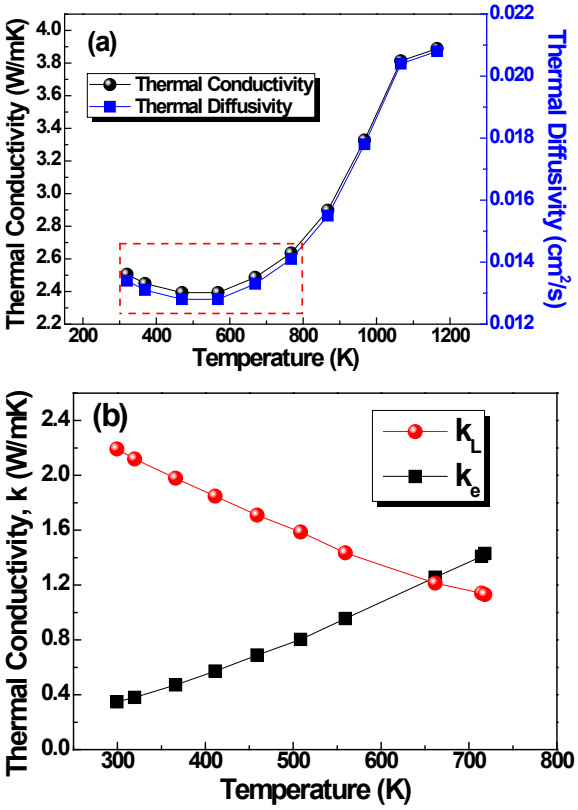

Fig. 5. Temperature dependence of the (a) thermal diffusivity and thermal conductivity and (b) electronic and lattice thermal conductivity of $Hf_{0.25}Zr_{0.25}Ti_{0.5}NiSn_{0.998}Sb_{0.002}$ sample.

in carrier mobility with rising temperature. Considering the temperature dependence of the electrical conductivity within the variable-range hopping model [13], the electrical conductivity is given by $\sigma=A\exp[-(T_0/T)^{1/4}]$, where A and T_0 are constants. As shown in Fig. 2(b), the plot of ln σ vs. $T^{1/4}$ shows a clear linear behavior, indicating polaron hopping conduction. In addition, it is believed that Sb-doping into Sn sites in the $Hf_{0.25}Zr_{0.25}Ti_{0.5}NiSn_{0.998}Sb_{0.002}$ composition also increased the electrical conductivity due to introduction of a charge carrier [14].

Figure 3 shows the temperature dependence of the Seebeck coefficent, α. The negative α value of the $Hf_{0.25}Zr_{0.25}Ti_{0.5}NiSn_{0.998}Sb_{0.002}$ compound indicates that it is an *n*-type semiconductor. |α| increases with the increase in temperature from RT, and reaches a maximum of 213 μV/K at about 550 K, which is due to the increase in the effective density of states with increasing temperature in the nondegenerate semiconductor. This starts to decrease due to bipolar conduction by increased minority carrier. However, the variation is not significant, and, thus, may be caused by the polaron hopping conduction and/or the increase in carrier concentration by thermal excitation.

The power factor (PE), as calculated by the electrical conductivity and Seebeck coefficient under a given temperature range, $PE = \sigma\alpha^2$ for the $Hf_{0.25}Zr_{0.25}Ti_{0.5}NiSn_{0.998}Sb_{0.002}$ compound, is shown in Fig. 4. The PE increased with increasing temperature, because both the electrical conductivity and Seebeck coefficient increased by nondegenerate semiconducting behavior. As a result, we obtained the maximum PE value of 33.98×10^{-4} W/mK^2 at about 700 K.

Thermal conductivity plays an important role that directly affects the figure of merit and, thereby, the energy conversion efficiency of thermoelectric materials. The thermal conductivity of a material is the sum of the two contributions: the electronic thermal conductivity (k_e) and the lattice thermal conductivity (k_L). Therefore, $k=k_e+k_L$. Both components can be separated by the Wiedermann-Franz law [15]: $k_e=(\pi^2/3)(k_B/e)^2\sigma T=L\sigma T$, where k_B is Boltzmann's constant, e is the quantity of electronic charge for one electron, and L is the Lorenz number ($=2.45\times10^{-8}$ WΩK^{-2}). The thermal conductivity was calculated by multiplying the measured thermal diffusivity, density, and specific heat. Figure 5(a) shows the thermal conductivity depending on temperature in the range from RT to 1,118 K, which was calculated by using the thermal diffusivity data shown in Fig. 5(a). It can be seen that the thermal conductivity of the $Hf_{0.25}Zr_{0.25}Ti_{0.5}NiSn_{0.998}Sb_{0.002}$ compound was significantly reduced to a low value of 2.5 W/mK at RT. It is anticipated that the low thermal conductivity can be explained by mass fluctuation phonon scattering and/or strain field effects due to the substitution of (Hf,Zr) by Ti in crystal. The effect of the (Hf/Zr) substitution with Ti on thermal conductivity in the HH compounds has also been demonstrated in previous studies [12,14,16]. With increasing temperature, the total thermal conductivity increased above 500 K, as the electronic thermal conductivity increases dominantly (see Fig. 5(b)). The combination of low thermal conductivity and high power factor led to the maximum value of the dimensionless figure of merit, ZT = 0.94 at 718 K, as shown in Fig. 6. At high temperature, the downward Seebeck coefficient and the upward electronic thermal conduc-

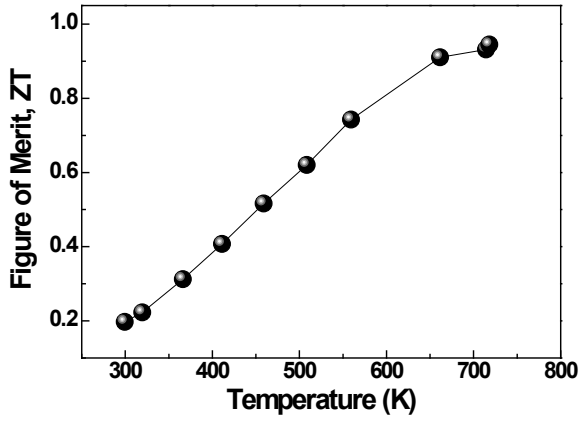

Fig. 6. Temperature dependence of the dimensionless figure of merit (ZT) of $Hf_{0.25}Zr_{0.25}Ti_{0.5}NiSn_{0.998}Sb_{0.002}$ sample from RT to 718 K.

tivity, which are related strongly to the majority carrier concentration, give rise to diminution of the uptrend in the figure of merit.

4. CONCLUSIONS

The *n*-type $Hf_{0.25}Zr_{0.25}Ti_{0.5}NiSn_{0.998}Sb_{0.002}$ Half-Heusler (HH) alloy composition was successfully synthesized using the induction melting method and SPS. The single phase of the Half-Heusler structure was achieved after annealing and the SPS processes. As the compound shows a nondegenerate semiconducting behavior, the dimensionless figure of merit increased with temperature and the maximum figure of merit, ZT = 0.94 at 718 K, was obtained by combining low thermal conductivity and the power factor, which was achieved using this composition.

ACKNOWLEDGMENT

This work was supported by the Industrial Technology Innovation Program (Industrial Materials Core Technology Development Program) funded by the Ministry of Trade, Industry and Energy, Republic of Korea (10052977).

REFERENCES

[1] F. J. Disalvo, *Science*, **285**, 703 (1999). [DOI: http://dx.doi.org/10.1126/science.285.5428.703]
[2] Z. C. Cai, P. Fan, Z. H. Zheng, P. J. Liu, T. B. Chen, J. T. Luo, G. X. Liang, and D. P. Zhang, *Appl. Surf. Sci.*, **280**, 225 (2013). [DOI: http://dx.doi.org/10.1016/j.apsusc.2013.04.138]
[3] B. C. Sales, D. Mandrus, R. K. Williams, *Science*, **272**, 1325 (1996). [DOI: http://dx.doi.org/10.1126/science.272.5266.1325]
[4] M. Scheele, N. Oeschler, K. Meier, A. Kornowski, C. Klinke, and H. Weller, *Adv. Funct. Mater.*, **19**, 3476 (2009). [DOI: http://dx.doi.org/10.1002/adfm.200901261]
[5] J. J. Shen, L. P. Hu, T. J. Zhu, and X. B. Zhao, *Appl. Phys. Lett.*, **99**, 124102 (2011). [DOI: http://dx.doi.org/10.1063/1.3643051]
[6] V. Kuznetsov, L. Kuznetsova, A. Kaliazin, and D. Rowe, *J. Mater. Sci.*, **37**, 2893 (2002). [DOI: http://dx.doi.org/10.1023/A:1016092224833]
[7] Y. Gelbstein, Y. Rosenberg, Y. Sadia, and M. Dariel, *J. Phys. Chem. C*, **114**, 13126 (2010). [DOI: http://dx.doi.org/10.1021/jp103697s]
[8] K. Biswas, J. He, G. Wang, S. H. Lo, C. Uher, V. P. Dravid, and M. G. Kanatzidis, *Energy Environ. Sci.*, **4**, 4675 (2011). [DOI: http://dx.doi.org/10.1039/c1ee02297k]
[9] S. N. Girard, J. He, X. Zhou, D. Shoemaker, C. M. Jaworski, C. Uher, V. P. Dravid, J. P. Heremans, and M. G. Kanatzidis, *J. Am. Chem. Soc.*, **133**, 16588 (2011). [DOI: http://dx.doi.org/10.1021/ja206380h]
[10] S. Ballikaya, N. Uzar, S. Yildirim, J. R. Salvador, and C. Uher, *J. Solid State Chem.*, **193**, 31 (2012). [DOI: http://dx.doi.org/10.1016/j.jssc.2012.03.029]
[11] G. Rogl, A. Grytsiv, M. Falmbigl, E. Bauer, C. Mangler, C. Rentenberger, M. Zehetbauer, and P. Rogl, *Acta Mater.*, **60**, 4487 (2012). [DOI: http://dx.doi.org/10.1016/j.actamat.2012.04.038]
[12] S. Sakurada and N. Shutoh, *Appl. Phys. Lett.*, **86**, 082105 (2005). [DOI: http://dx.doi.org/10.1063/1.1868063]
[13] N. F. Mott, *Metal-Insulator Transitions* (Taylor and Francis, London, 1974).
[14] M. Schwall and B. Balke, *Phys. Chem. Phys.*, **15**, 1870 (2013).
[15] G. Wiedermann and R. Franz, *Ann. Phys. Lpz.*, **89**, 497 (1853).
[16] N. Shutoh and S. Sakurada, *J. Alloys Compd.*, **389**, 204 (2005). [DOI: http://dx.doi.org/10.1016/j.jallcom.2004.05.078]